one proposed by Sahashi *et al.*[22] Although the reason why this occurred is unknown, this case tells us that the exact nature of aberrant splicing resulting from splice site mutations is unlikely to be predicted. Therefore, an RNA analysis such as RT-PCR is indispensable in the detection of abnormal mRNA if a mutation that potentially affects RNA splicing is identified.

ACKNOWLEDGEMENTS

We are indebted to the patients who participated in this study. We also thank Hiromi Hatsuse for excellent technical assistance.

1 Gorlin, R. J. & Goltz, R. W. Multiple nevoid basal-cell epithelioma, jaw cysts and bifid rib. A syndrome. *N. Engl. J. Med.* **262,** 908–912 (1960).
2 Evans, D. G. R., Ladusan, E. J., Rimmer, S., Burnell, L. D., Thakker, N. & Farndon, P. A. Complications of the nevoid basal cell carcinoma syndrome: results of the population based study. *J. Med. Genet.* **30,** 460–464 (1993).
3 Shanley, S., Ratcliffe, J., Hockey, A., Haan, E., Oley, C., Ravine, D. *et al.* Nevoid basal cell carcinoma syndrome: review of 118 affected individuals. *Am. J. Med. Genet.* **50,** 282–290 (1994).
4 Hahn, H., Wicking, C., Zaphiropoulous, P. G., Gailani, M. R., Shanley, S., Chidambaram, A. *et al.* Mutations of the human homolog of Drosophila patched in the nevoid basal cell carcinoma syndrome. *Cell* **85,** 841–851 (1996).
5 Johnson, R. L., Rothman, A. L., Xie, J., Goodrich, L. V., Bare, J. W., Bonifas, J. M. *et al.* Human homolog of patched, a candidate gene for the basal cell nevus syndrome. *Science* **272,** 1668–1671 (1996).
6 Fujii, K., Kohno, Y., Sugita, K., Nakamura, M., Moroi, Y., Urabe, K. *et al.* Mutations in the human homologue of *Drosophila patched* in Japanese nevoid basal cell carcinoma syndrome patients. *Hum. Mutat.* **21,** 451–452 (2003).
7 Taicher, S. & Shteyer, A. The basal cell nevus syndrome associated with cleft lip and cleft palate: report of case. *J. Oral. Surg.* **36,** 799–802 (1978).
8 Soekarman, D., Fryns, J. P., Casaer, P. & Van Den Berghe, H. Increased head circumference and facial cleft as presenting signs of the nevoid basal-cell carcinoma syndrome. *Genet. Couns.* **2,** 157–162 (1991).
9 Lambrecht, J. T. & Kreusch, T. Examine your orofacial cleft patients for Gorlin–Goltz syndrome. *Cleft. Palate. Craniofac. J.* **34,** 342–350 (1997).
10 van Dijk, E. & Neering, H. The association of cleft lip and palate with basal cell nevus syndrome. *Oral. Surg. Oral. Med. Oral. Pathol.* **50,** 214–216 (1980).
11 Mansilla, M. A., Cooper, M. E., Goldstein, T., Castilla, E. E., Lopez Camelo, J. S., Marazita, M. L. *et al.* Contributions of PTCH gene variants to isolated cleft lip and palate. *Cleft. Palate. Craniofac. J.* **43,** 21–29 (2006).
12 Noordhoff, M. S. & Chen, P. K. *Unilateral Cheiloplasty-Plastic Surgery* 2nd edn (Saunders, Philadelphia, 2006).
13 Ahn, S. G., Lim, Y. S., Kim, D. K., Kim, S. G., Lee, S. H. & Yoon, J. H. Nevoid basal cell carcinoma syndrome: a retrospective analysis of 33 affected Korean individuals. *Int. J. Oral. Maxillofac. Surg.* **33,** 458–462 (2004).
14 McCarthy, J. G., Cutting, C. B. & Hogan, V. M. *Introduction to Facial Clefts—Plastic Surgery* (Saunders, Philadelphia, 1990).
15 Kimonis, V. E., Goldstein, A. M., Pastakia, B., Yang, M. L., Kase, R., DiGiovanna, J. J. *et al.* Clinical manifestations in 105 persons with nevoid basal cell carcinoma syndrome. *Am. J. Med. Genet.* **69,** 299–308 (1997).
16 Breathnach, R. & Chambon, P. Organization and expression of eukaryotic split genes coding for proteins. *Annu. Rev. Biochem.* **50,** 349–383 (1981).
17 Morgan, T. A., Burton, C. C. & Qian, F. A retrospective review of treatment of the odontogenic keratocyst. *J. Oral. Maxillofac. Surg.* **63,** 635–639 (2005).
18 Philipsen, H. P. Keratocystic odontogenic tumour. in *World Health Organization Classification of Tumours. Pathology and Genetics of Head and Neck Tumours* (eds Barnes, L., Eveson, J.W., Reichart, P.A. & Sidransky, D.) 306–307 (IARC Press: Lyon, 2005).
19 van den Boogaard, M. J., Dorland, M., Beemer, F. A. & van Amstel, H. K. MSX1 mutation is associated with orofacial clefting and tooth agenesis in humans. *Nat. Genet.* **24,** 342–343 (2000).
20 Zucchero, T. M., Cooper, M. E., Maher, B. S., Daack-Hirsch, S., Nepomuceno, B., Ribeiro, L. *et al.* Interferon regulatory factor 6 (IRF6) gene variants and the risk of isolated cleft lip or palate. *N. Engl. J. Med.* **351,** 769–780 (2004).
21 Hu, D. & Helms, J. A. The role of sonic hedgehog in normal and abnomal craniofacial morphogenesis. *Development* **126,** 281–292 (1999).
22 Sahashi, K., Masuda, A., Matsuura, T., Shinmi, J., Zhang, Z. & Takeshima, Y. *In vitro* and in silico analysis reveals an efficient algorithm to predict the splicing consequences of mutations at the 5′ splice sites. *Nucleic. Acids. Res.* **35,** 5995–6003 (2007).

RESEARCH LETTER

AMERICAN JOURNAL OF
medical genetics

A de novo 1.9-Mb Interstitial Deletion of 3q13.2q13.31 in a Girl With Dysmorphic Features, Muscle Hypotonia, and Developmental Delay

Keiko Shimojima,[1]* Kayoko Saito,[2] and Toshiyuki Yamamoto[1]

[1]International Research and Educational Institute for Integrated Medical Sciences (IREIIMS), Tokyo Women's Medical University, Tokyo, Japan

[2]Institute of Medical Genetics, Tokyo Women's Medical University, Tokyo, Japan

Received 20 November 2008; Accepted 14 May 2009

TO THE EDITOR:

Constitutional interstitial deletions of the proximal long arm of chromosome 3 are rare. In 2008, Simovich et al. reported a 20-month-old Hispanic male with a 2.5-Mb de novo deletion of 3q13.11q13.12 with dysmorphic features, minor peripheral skeletal abnormalities, and a heart defect. Including this, there have been only 12 patients reported [Arai et al., 1982; Jenkins et al., 1985; McMorrow et al., 1986; Okada et al., 1987; Fujita et al., 1992; Genuardi et al., 1994; Ogilvie et al., 1998; Hou, 2004; Kosaki et al., 2005; Lawson-Yuen et al., 2006; Sato et al., 2007; Simovich et al., 2008]. The deleted segments vary in region and size and have different breakpoints, making the genotype and phenotype correlation very difficult. Recently, we encountered a new patient with chromosomal deletion of 3q13.2q13.31, which was identified by array-based comparative genomic hybridization (aCGH). In comparison the phenotype of this patient to the previously reported patients with deletion of this region, muscle hypotonia and developmental delay are the only common findings.

FIG. 1. The patient with del(3)(q13.2q13.31) at 3 years old. [Color figure can be viewed in the online issue, which is available at www.interscience.wiley.com.]

How to Cite this Article:
Shimojima K, Saito K, Yamamoto T. 2009. A de novo 1.9-Mb interstitial deletion of 3q13.2q13.31 in a girl with dysmorphic features, muscle hypotonia, and developmental delay.
Am J Med Genet Part A 149A:1818–1822.

A 4-year and 11-month-old girl was born at 39 weeks and 2 days of gestation by vaginal delivery as the second child of a 36-year-old father and a 35-year-old mother. Her older brother and younger sister were healthy. There was a past history of a spontaneous abortion after the birth of the first child. The proposita's birth weight was 2,688 g (25th centile), length was 47.5 cm (25th centile), and head circumference was 33.5 cm (75th centile). Developmental milestones were as follows: head control at 3 months, sitting unaided at 1 year and 1 month, crawling at 1 year and 6 months, and walking without support at 2 years of age. At 10 months, she suffered a febrile seizure complicated with a continuous convulsion

Additional supporting information may be found in the online version of this article.

Grant sponsor: Special Coordination Funds for Promoting Science and Technology, Ministry of Education, Culture, Sports, Science and Technology (Japan).

*Correspondence to:
Keiko Shimojima, M.D., International Research and Educational Institute for Integrated Medical Sciences (IREIIMS), Tokyo Women's Medical University, 8-1 Kawada-cho, Shinjuku-ward, Tokyo 162-8666, Japan.
E-mail: shimojima@imcir.twmu.ac.jp

Published online 16 July 2009 in Wiley InterScience (www.interscience.wiley.com)
DOI 10.1002/ajmg.a.32963

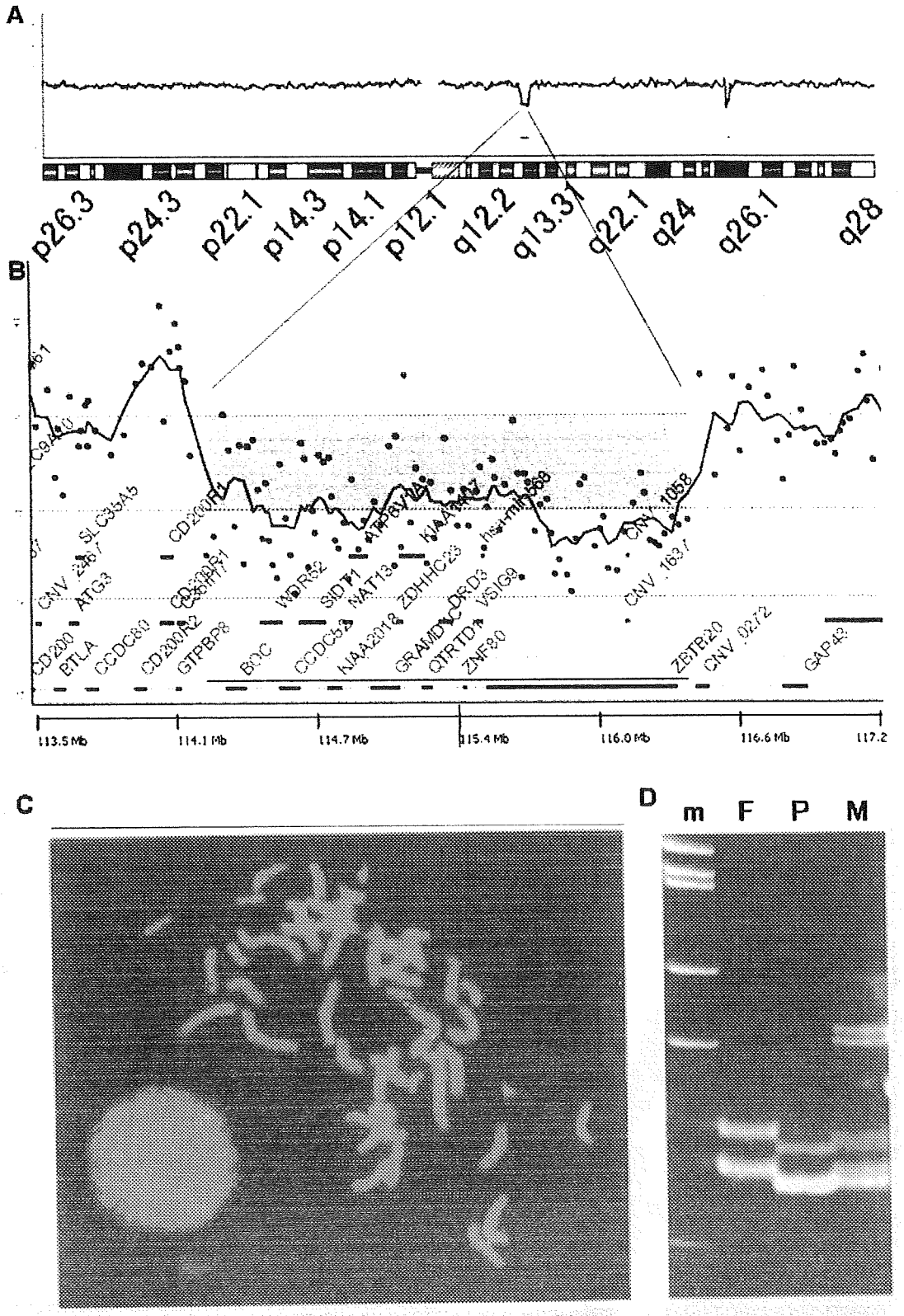

FIG. 2. The results of laboratory examination. A: aCGH data are shown using CGH Analytics version 3.5 in Chromosomal Views. The aberrant area is indicated by a gray rectangle. B: The aberrant area of chromosome 3q13.2q13.3 is expanded in Gene Views. A 1.9-Mb deletion was shown by a gray rectangle. C: Two-color FISH analysis using a combination of the BAC clones RP11-6301 (red) and RP11-2405 (green) as probes. A single green signal indicates the deletion of this region on one chromosome. D: Linkage analysis of D3S1310 separated on a polyacrylamide gel and visualized by ethidium bromide staining. The bands of the present patient are common only with those of the mother. m, molecular size marker; P, patient; F, father; M, mother. [Color figure can be viewed in the online issue, which is available at www.interscience.wiley.com.]

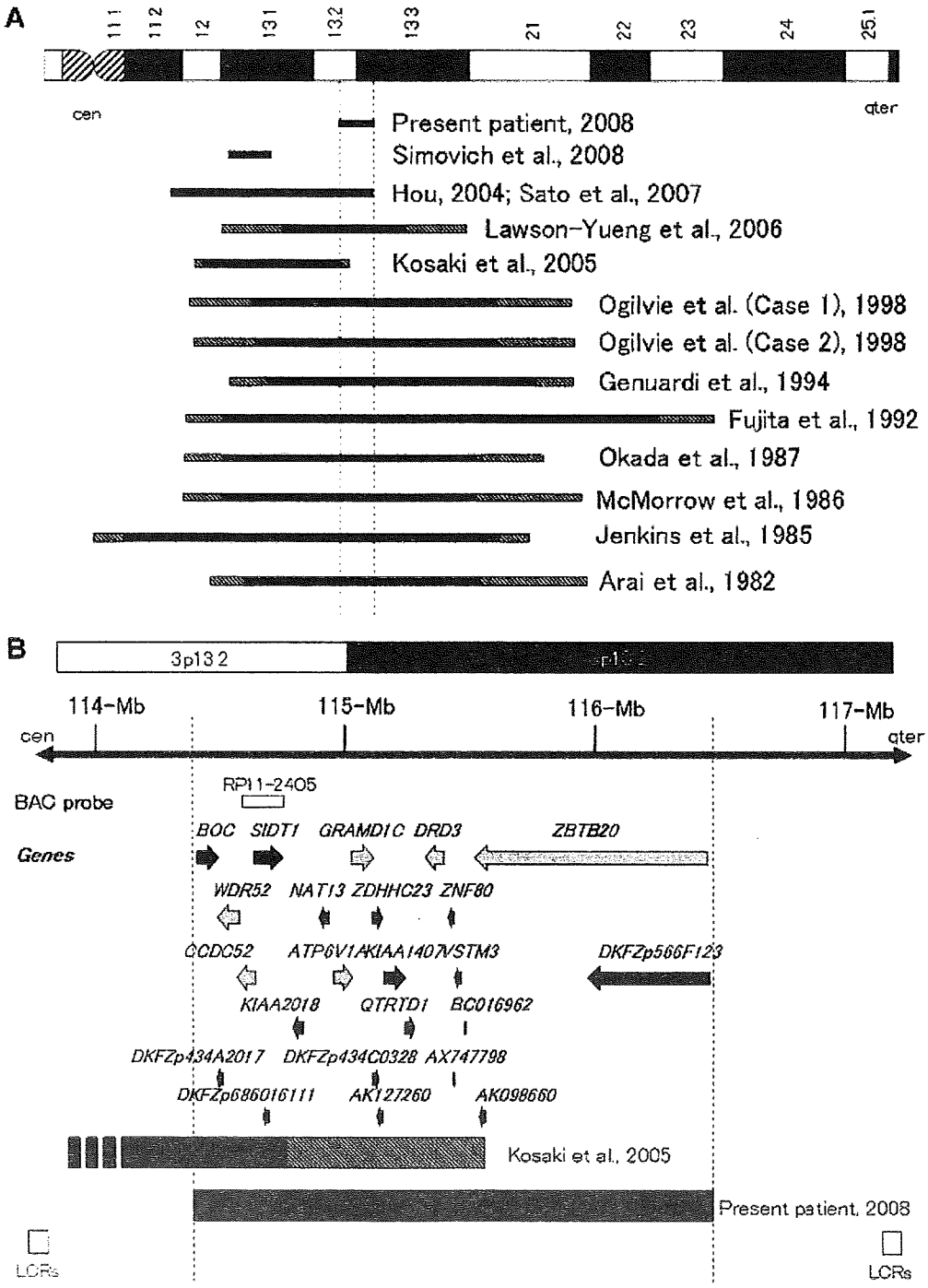

FIG. 3. Physical maps of the 3q13 region. Deletion regions with the size of each deletion (A), and gene mapping of the 1.9-Mb deletion region of the present patient (B). Horizontal black bars and diagonally-lined rectangles indicate deletion regions and fuzzy regions, respectively. White rectangles; BAC probes used in this study, black arrows; the position and the direction of the genes located in this area, gray arrows; gene insertions or deletions already reported in the database of Genomic Variants (Human Genome Segmental Duplication Database: http://projects.tcag.ca/humandup/).

over a period of 1 hr triggered by an upper airway infection. Radiological examination, including brain magnetic resonance imaging, echocardiogram, and abdominal echocardiography, showed no abnormality. Electroencephalogram, auditory and ophthalmologic assessments also showed no abnormality at that time.

At 3 years and 2 months, she was referred to us for the clinical evaluation of dysmorphic features, muscle hypotonia, and developmental delay including markedly dysarthric speech. Her growth was normal, with a height of 94.6 cm (75th centile), weight of 13.8 kg (50th centile), and head circumference of 49.5 cm (75th centile). Clinical examination revealed generalized hypotonia, joint hyperlaxity, valgus feet, and dysmorphic features, including craniofacial abnormalities of ptosis, bilateral epicanthal folds, depressed nasal root/bridge, and bulbous anteverted nose (Fig. 1). There was no abnormality of the cranial nerves or deep tendon reflexes. DQ was 60: postural-motor [P-M] 50; cognitive-adaptive [C-A] 62; and language-social [L-S] 58, using Revised Kyoto Scale of Psychological Development (Revised-KSPD) [Kono et al., 2008].

As conventional chromosomal examination showed a normal female karyotype, we performed aCGH using Human Genome CGH Microarray 105A (Agilent Technologies, Palo Alto, CA) according to the manufacturer's protocol, with genomic DNA extracted from peripheral blood using the QIAquick DNA extraction kit (QIAGEN, Hilden, Germany). Genomic copy number aberrations were visualized using the ADM-II algorithm in CGH analytics version 3.5 (Agilent Technologies). A loss of the genomic copy number at 3q13.2q13.31 (114,321,633//116,406,833) with a deletion size of 1.9-Mb was identified (Fig. 2A,B), and, subsequently, fluorescence in situ hybridization (FISH) was performed according to a method described elsewhere [Paez et al., 2008]. The BAC clones RP11-63O1, RP11-24O5, and RP11-342J15 were selected from the in silico library Build 2006 (UCSC Human genome browser: http//genome.ucsc. edu/cgi-bin/hgGateway). The result of FISH analysis reconfirmed the chromosomal deletion (Fig. 2C). The same FISH analyses performed on her parents confirmed no deletion in either parent, indicating a de novo deletion in the proposita. To confirm the parental origin of the deletion, the dinucleotide repeat polymorphism on the deletion region, D3S1310 (located on 3q13.31: 116,265,127-116,265,478) was analyzed using a method described elsewhere [Paez et al., 2008]. The patient shared the allele only common with that of the mother (Fig. 2D). This means that the paternal allele had been deleted. The final diagnosis was arr 3q13.2q13.31(114,321,633-116,406,833) × 1.ish del(3)(q13.2q13.31)(RP11-24O5×1, RP11-342J15×1) dn.

Clinical data from this patient and the previously reported 12 patients with 3q13 deletion are summarized in supporting information Table I (supporting information Table I may be found in the online version of this article). This 1.9-Mb deletion region completely overlapped with that of 10 patients, and the partial 1-Mb deletion region overlapped with that reported by Kosaki et al. [2005] (Fig. 3A). The interstitial deletion of 3q13 has been associated with a wide range of phenotypes. As the number of patients is still insufficient, clinically recognized phenotypes have not been established yet. The 1.9-Mb deletion in this patient was the smallest deletion among the reported cases with interstitial deletion of 3q13.

Simovich et al. [2008] suggested that *ALCAM* and *CBLB* located on 3q13.11q13.12 are crucial for the development of craniofacial abnormalities, including a prominent forehead, hypertelorism, anteverted nose, and ear malformation. Since the 2.5-Mb deletion region in the patient reported by Simovich et al. [2008] does not overlap with that of our patient, it is reasonable that the facial gestalt of the patient reported by Simovich et al. [2008] was not similar to our patient.

In the 11 previously reported patients with the deletion of 13q13.2 region, the patient reported by Lawson-Yuen et al. [2006] showed prominent hypotonia. Although there is no clear description of hypotonia, the other three patients showed feeding difficulty, dyspnea, tachypnea, joint contractures, and talipes equinovarus, which may be the consequence of hypotonia. Thus, muscle hypotonia and developmental delay could be common findings in the 11 patients with the overlapping 1-Mb proximal 3q deletion. In this segment there are 23 known genes (Build 2006) (Fig. 3B and supporting information Table I (supporting information Table I may be found in the online version of this article)), and some of them are candidate genes for the symptoms of the presenting patient. One of them is brother of CDON gene (*BOC*) (OMIM 608708). Because cell adhesion molecule-related/downregulated by oncogenes (*CDON*) on 11q14.2 and *BOC* on 13q13.2 mediates cell–cell interactions between muscle precursor cells and promotes the differentiation of myogenic cells [Kang et al., 2002, 2003], *BOC* might be responsible for the muscle hypotonia in the presenting patient. Another is *DRD3*, the dopamine receptor D3 gene, encoding the D3 subtype of the five (D1–D5) dopamine receptors. This receptor is localized to the limbic areas of the brain, and function for locomotion, cognition, emotion, and affect as well as neuroendocrine secretion [Niznik and Van Tol, 1992; Accili et al., 1996; Missale et al., 1998]. Recently, many association studies in patients with neuro-psychiatric disorders have explored the contribution of *DRD3* variants to their phenotype [Hoenicka et al., 2007; Beninger and Banasikowski, 2008]. In 1996, Accili et al. generated mice lacking functional *DRD3*, and homozygous mice lacking *DRD3* displayed increased locomotor activity and rearing behavior, and heterozygous mice showed similar but less pronounced behavioral alterations [Accili et al., 1996]. Although the presenting patient does not show any behavioral abnormality, neurological symptoms including developmental delay and dysarthria noted in this patient might be derived from haploinsufficiency of *DRD3*.

In this deletion region, there are some other genes, which are highly expressed in the brain, including *CCDC52*, *SIDT1*, *ATP6V1A*, *ZNF80*, and *ZBTB20*, which may also be correlated with the phenotype of deletion 3q13.2q13.3.

ACKNOWLEDGMENTS

This work was supported by the International Research and Educational Institute for Integrated Medical Sciences, Tokyo Women's Medical University, which is supported by the Program for Promoting the Establishment of Strategic Research Centers, Special Coordination Funds for Promoting Science and Technology, Ministry of Education, Culture, Sports, Science and Technology (Japan).

REFERENCES

Accili D, Fishburn CS, Drago J, Steiner H, Lachowicz JE, Park BH, Gauda EB, Lee EJ, Cool MH, Sibley DR, Gerfen CR, Westphal H, Fuchs S. 1996. A targeted mutation of the D3 dopamine receptor gene is associated with hyperactivity in mice. Proc Natl Acad Sci USA 93: 1945–1949.

Arai K, Matukiyo H, Takazawa H. 1982. A case report of partial deletion of the long arm of the No.3 chromosome. Med Genet Res 4:1–4.

Beninger RJ, Banasikowski TJ. 2008. Dopaminergic mechanism of reward-related incentive learning: Focus on the dopamine D(3) receptor. Neurotox Res 14:57–70.

Fujita H, Meng J, Kawamura M, Tozuka N, Ishii F, Tanaka N. 1992. Boy with a chromosome del(3)(q12q23) and blepharophimosis syndrome. Am J Med Genet 44:434–436.

Genuardi M, Calvieri F, Tozzi C, Coslovi R, Neri G. 1994. A new case of interstitial deletion of chromosome 3q, del(3q)(q13.12q21.3), with agenesis of the corpus callosum. Clin Dysmorphol 3:292–296.

Hoenicka J, Aragues M, Ponce G, Rodriguez-Jimenez R, Jimenez-Arriero MA, Palomo T. 2007. From dopaminergic genes to psychiatric disorders. Neurotox Res 11:61–72.

Hou JW. 2004. Congenital arhinia with de novo reciprocal translocation, t(3;12)(q13.2;p11.2). Am J Med Genet Part A 130A:200–203.

Jenkins MB, Stang HJ, Davis E, Boyd L. 1985. Deletion of the proximal long arm of chromosome 3 in an infant with features of Turner syndrome. Ann Genet 28:42–44.

Kang JS, Mulieri PJ, Hu Y, Taliana L, Krauss RS. 2002. BOC, an Ig superfamily member, associates with CDO to positively regulate myogenic differentiation. EMBO J 21:114–124.

Kang JS, Feinleib JL, Knox S, Ketteringham MA, Krauss RS. 2003. Promyogenic members of the Ig and cadherin families associate to positively regulate differentiation. Proc Natl Acad Sci USA 100: 3989–3994.

Kono Y, Mishina J, Sato N, Watanabe T, Honma Y. 2008. Developmental characteristics of very low-birthweight infants at 18 months' corrected age according to birthweight. Pediatr Int 50:23–28.

Kosaki R, Fukuhara Y, Kosuga M, Okuyama T, Kawashima N, Honna T, Ueoka K, Kosaki K. 2005. OEIS complex with del(3)(q12.2q13.2). Am J Med Genet Part A 135A:224–226.

Lawson-Yuen A, Berend SA, Soul JS, Irons M. 2006. Patient with novel interstitial deletion of chromosome 3q13.1q13.3 and agenesis of the corpus callosum. Clin Dysmorphol 15:217–220.

McMorrow LE, Reid CS, Coleman J, Medeiros A, D'Andrea M, Santucci T. 1986. A new interstitial deletion of the long arm of choromosome 3. Am J Hum Genet 39:A124.

Missale C, Nash SR, Robinson SW, Jaber M, Caron MG. 1998. Dopamine receptors: From structure to function. Physiol Rev 78:189–225.

Niznik HB, Van Tol HH. 1992. Dopamine receptor genes: New tools for molecular psychiatry. J Psychiatry Neurosci 17:158–180.

Ogilvie CM, Rooney SC, Hodgson SV, Berry AC. 1998. Deletion of chromosome 3q proximal region gives rise to a variable phenotype. Clin Genet 53:220–222.

Okada N, Hasegawa T, Osawa M, Fukuyama Y. 1987. A case of de novo interstitial deletion 3q. J Med Genet 24:305–308.

Paez MT, Yamamoto T, Hayashi K, Yasuda T, Harada N, Matsumoto N, Kurosawa K, Furutani Y, Asakawa S, Shimizu N, Matsuoka R. 2008. Two patients with atypical interstitial deletions of 8p23.1: Mapping of phenotypical traits. Am J Med Genet Part A 146A:1158–1165.

Sato D, Shimokawa O, Harada N, Olsen OE, Hou JW, Muhlbauer W, Blinkenberg E, Okamoto N, Kinoshita A, Matsumoto N, Kondo S, Kishino T, Miwa N, Ariga T, Niikawa N, Yoshiura K. 2007. Congenital arhinia: Molecular-genetic analysis of five patients. Am J Med Genet Part A 143A:546–552.

Simovich MJ, Bland SD, Peiffer DA, Gunderson KL, Cheung SW, Yatsenko SA, Shinawi M. 2008. Delineation of the proximal 3q microdeletion syndrome. Am J Med Genet Part A 146A:1729–1735.

ELSEVIER

Brain & Development 32 (2010) 171–179

BRAIN & DEVELOPMENT
Official Journal of the Japanese Society of Child Neurology

www.elsevier.com/locate/braindev

Original article

Comprehensive genetic analyses of *PLP1* in patients with Pelizaeus–Merzbacher disease applied by array-CGH and fiber-FISH analyses identified new mutations and variable sizes of duplications

Keiko Shimojima [a], Takehiko Inoue [b], Ai Hoshino [c,d], Satsuki Kakiuchi [e], Yoshiaki Watanabe [f], Masayuki Sasaki [g], Akira Nishimura [g], Akiko Takeshita-Yanagisawa [h], Go Tajima [i], Hiroshi Ozawa [c,j], Masaya Kubota [c,k], Jun Tohyama [l], Masayuki Sasaki [m], Akira Oka [k,n], Kayoko Saito [o], Makiko Osawa [h], Toshiyuki Yamamoto [a,*]

[a] *International Research and Educational Institute for Integrated Medical Sciences (IREIIMS), Tokyo Women's Medical University, 8-1 Kawada-cho, Shinjuku-ward, Tokyo 162-8666, Japan*
[b] *Division of Child Neurology, Institute of Neurological Sciences, Faculty of Medicine, Tottori University, Yonago, Japan*
[c] *Department of Pediatrics, Tokyo Metropolitan Hachioji Children's Hospital, Hachioji, Japan*
[d] *Department of Neuropediatrics, Tokyo Metropolitan Neurological Hospital, Fuchu, Japan*
[e] *Department of Neonatology, Tokyo Metropolitan Bokutoh Hospital, Tokyo, Japan*
[f] *Department of Child Neurology, Okayama University Graduate School of Medicine, Okayama, Japan*
[g] *Department of Pediatrics, Kyoto Prefectural University of Medicine, Kyoto, Japan*
[h] *Department of Pediatrics, Faculty of Medicine, Tokyo Women's medical University, Tokyo, Japan*
[i] *Department of Pediatrics, Hiroshima University Graduate School of Biomedical Sciences, Hiroshima, Japan*
[j] *Shimada Ryoiku Center, Tama, Japan*
[k] *Division of Child Neurology, National Center of Child Health and Development, Tokyo, Japan*
[l] *Epilepsy Center, National Nishi-Niigata Chuo National Hospital, Niigata, Japan*
[m] *Department of Child Neurology, National Center Hospital for Mental, Nervous and Muscular Disorders, National Center of Neurology and Psychiatry, Kodaira, Japan*
[n] *Department of Pediatrics, Faculty of Medicine, The University of Tokyo, Tokyo, Japan*
[o] *Institute of Medical Genetics, Tokyo Women's medical University, Tokyo, Japan*

Received 22 November 2008; received in revised form 2 February 2009; accepted 22 February 2009

Abstract

Pelizaeus–Merzbacher disease (PMD; MIM#312080) is a rare X-linked recessive neurodegenerative disorder. The main cause of PMD is alterations in the proteolipid protein 1 gene (*PLP1*) on chromosome Xq22.2. Duplications and point mutations of *PLP1* have been found in 70% and 10–25% of all patients with PMD, respectively, with a wide clinical spectrum. Since the underlining genomic abnormalities are heterogeneous in patients with PMD, clarification of the genotype-phenotype correlation is the object of this study. Comprehensive genetic analyses using microarray-based comparative genomic hybridization (aCGH) analysis and genomic sequencing were applied to fifteen unrelated male patients with a clinical diagnosis of PMD. Duplicated regions were further analyzed by fiber-fluorescence *in situ* hybridization (FISH) analysis. Four novel and one known nucleotide alterations were identified in five patients. Five microduplications including *PLP1* were identified by aCGH analysis with the sizes ranging from

* Corresponding author. Tel.: +81 3 3353 8111; fax: +81 3 3352 3088
E-mail address: yamamoto@imcir.twmu.ac.jp (T. Yamamoto).

0387-7604/$ - see front matter
doi:10.1016/j.braindev.2009.02.011

374 to 951-kb. The directions of five *PLP1* duplications were further investigated by fiber-FISH analysis, and all showed tandem duplications. The common manifestations of the disease in patients with *PLP1* mutations or duplications in this study were nystagmus in early infancy, dysmyelination revealed by magnetic resonance imaging (MRI), and auditory brain response abnormalities. Although the grades of dysmyelination estimated by MRI findings were well correlated to the clinical phenotypes of the patients, there is no correlation between the size of the duplications and the phenotypic severity.

Keywords: Array-based comparative genomic hybridization (aCGH); Fiber-FISH; Fluorescence *in situ* hybridization (FISH); Pelizaeus–Merzbacher disease (PMD); Proteolipid protein 1 (*PLP1*)

1. Introduction

Pelizaeus–Merzbacher disease (PMD; MIM#312080) is a rare X-linked recessive neurodegenerative disorder characterized by early onset nystagmus and hypotonia later evolving into spastic tetraparesis, dystonia, ataxia, and developmental delay usually beginning in the first year [1–3]. The main cause of PMD is alterations in the proteolipid protein 1 gene (*PLP1*; MIM#300401) on chromosome Xq22.2 [4–6], which encodes 2 proteins, PLP1 and the splicing variant, DM20, both of which are abundantly expressed in oligodendrocytes [3]. PLP1 is thought to play a major role in myelin sheath formation by promoting sheath compaction [7]. Within the heterogeneous group of dysmyelinating disorders, PMD accounts for 6.5% of all cases [8].

It has been proposed that patients with *PLP1*-related inherited dysmyelinating disorders should be clinically divided into 3 subgroups in order of decreasing severity: connatal, classic, and X-linked spastic paraplegia type 2 (SPG2; MIM#312920) [9]. Duplications of *PLP1* can be found in up to 70% of all patients with PMD, indicating that increased *PLP1* dosage is deleterious for normal myelination [10,11]. Point mutations in *PLP1* have been found in 10–25% of PMD cases with the entire clinical spectrum [11], ranging from the most severe connatal form to the least severe SPG2 form, depending on the affected domain of the protein [9]. Although there are characteristic clinical and radiological features of PMD [1,12], molecular and/or cytogenetic analyses are necessary for final diagnosis because *PLP1* is only expressed in the central nervous system and there are no practical biochemical tests available. The first step in genetic testing should be a genomic dosage analysis of *PLP1* because the major genetic aberration is duplication of *PLP1*. For this purpose, various methods have been used, including southern blotting [6], quantitative polymerase chain reaction (PCR) [13], fluorescence *in situ* hybridization (FISH) [14], multiplex ligation-dependent probe amplification (MLPA) [15], and multiplex amplifiable probe hybridization (MAPH) [16]. Recently, microarray-based comparative genome hybridization (aCGH) has emerged as a novel technology that enables detection and determination of the size of the duplicated or deleted genomic intervals [17]. In case of normal dosage of *PLP1*, nucleotide sequences of *PLP1* should be examined [18]. Here, we report our recent studies to develop comprehensive molecular and cytogenetic analyses to diagnose patients with PMD and to understand the pathogenic mechanism of PMD and its correlation between clinical phenotypes.

2. Materials

Fifteen unrelated male patients (age span from 1 year to 20 years old) with congenital dysmyelination were referred to us for genetic diagnosis based on the clinical diagnosis as PMD. Clinical information and radiographic findings by magnetic resonance imaging (MRI) for the patients were obtained from attending doctors. Based on the approval by the ethics committee at the institution, informed consents were obtained from patient's families, and peripheral blood samples were obtained from all patients. Lymphoblast cell lines were established from lymphocytes extracted from peripheral blood samples by immortalization with Epstein-Barr virus. Three of the fifteen patients (P1, P3, P4) had been diagnosed as having *PLP1* duplications by previously performed comparative PCR amplification method (data not shown).

Genomic DNAs of the patients were extracted from peripheral blood samples using the QIAquick DNA Extraction Kit (QIAGEN, Hamburg, Germany). Metaphase or prometaphase chromosomes were prepared from phytohemagglutinin-stimulated peripheral blood lymphocytes or lymphocyte cell lines according to standard techniques.

One extra cell line (S1) that showed duplication of Xp22.31 including steryl-sulfatase precursor gene (*STS*) as determined by aCGH, was derived from a non-PMD mentally retarded patient and used for fiber-FISH analysis as a positive control of *STS* duplication.

Population-based control DNA samples were obtained from 100 healthy Japanese volunteers.

3. Methods

3.1. aCGH analysis

aCGH analysis, using the Human Genome CGH Microarray 105A chip (Agilent Technologies, Santa

Clara, CA), was performed according to the manufacturer's instructions [19]. The data was extracted with Feature Extraction version 9 (Agilent Technologies) and visualized by CGH Analytics version 3.5 (Agilent Technologies). Statistically significant aberrations were determined using the ADM-II algorithm in CGH Analytics version 3.5 (Agilent Technologies).

3.2. Fiber-FISH analysis

Phytohemagglutinin-stimulated lymphocytes or lymphoblasts were harvested using a routine procedure that generates metaphase chromosomes and interphase nuclei. The fiber-FISH slides were prepared as follows: approximately 20 μl of cell suspensions containing metaphase and prometaphase chromosomes were pipetted onto a slide that was then dipped into a 10% sodium dodecyl sulfate (SDS) solution and removed slowly. Bacterial artificial chromosome (BAC) clones were selected from an in-silico library (UCSC Human genome browser, March 2006); RP4-540A13 and RP5-1055C14 mapped to the region surrounding *PLP1*, CTD-2171N231 and RP11-98J1 mapped to the *STS* region of Xp22.31. DNAs from the BAC clones were extracted using GenePrepStar PI-80X (Kurabo, Osaka, Japan), and labeled with digoxigenin-11-dUTP or biotin-16-dUTP (Roche Applied Science, Mannheim, Germany) by nick translation and denatured at 70 °C for 5 min. After hardening process with incubation at 65 °C for 150 min, the chromosome slides were denatured in 70% formamide/2× standard saline citrate (SSC) at 70 °C for 2 min, and then dehydrated at −20 °C in ethanol. The probe-hybridization mixture was applied on the chromosome slides and incubated at 37 °C for more than 16 h. The slides were then washed in 50% formamide/2× SSC at 37 °C for 12 min, 2× SSC at room temperature for 10 min, 1× SSC for 10 min, and 4× SSC for 10 min. And finally, the slides were incubated with 1% bovine serum albumin (BSA), 4× SSC, Fluorescein anti-biotin (Vector, Burlingame, CA, USA) and Anti-digoxigenin-rhodamine, Fab fragments (Roche) at 37 °C for 1 h. Slides were washed 3 times: in 4× SSC for 5 min, in 0.05% Triton-X-100/4× SSC for 5 min with shaking, and finally in 4× SSC for 5 min. The slides were then mounted in antifade solution containing 4′,6-diamino-2-phenylindole (DAPI) stain. Photomicroscopy was performed using a LICA CTR6000 microscope containing a quad filter set with single band excitation filters (Leica Microsystems, Tokyo, Japan).

3.3. PLP1 mutation analysis

The sequence of the patients' 7 coding exons of *PLP1* was determined using the neighboring intronic primers reported by Hobson et al. [20] and a BigDye Terminator Cycle Sequencing kit according to the manufacturer's protocol (Applied Biosystems, Foster City, CA). One hundred control samples were genotyped to verify that the *PLP1* mutation identified in the PMD patients was not found in the general population.

4. Results and discussion

4.1. Genetic diagnosis of PMD

Three distinct genetic mechanisms responsible for PMD have been reported: (1) Loss of PLP1 function caused by null mutations or deletions; (2) gain of toxic function (the PLP1 mutant protein accumulates in the endoplasmic reticulum, triggering increased oligodendrocyte cell death by apoptosis resulting in dysmyelination); (3) overexpression of PLP1 due to genomic duplication [3,7]. As mentioned in Section 2, three (P1, P3, and P4) of the 15 patients had been diagnosed as having *PLP1* duplications by previously performed comparative PCR amplification method, which were re-confirmed by aCGH and fiber-FISH in this study. Subsequently, two (P2 and P5) of the remaining twelve subjects were newly diagnosed as having *PLP1* duplications by aCGH. For the remaining ten patients without genomic duplications, we analyzed the genomic sequence of *PLP1* and identified three missense mutations, one splicing mutation, and one 3-bp deletion (Table 1). Thus, we were unable to determine genetic causes for the phenotype in the remaining five patients, and there is no patient who showed deletion of *PLP1*.

4.2. Detection of genomic duplications of PLP1 by aCGH

aCGH is a revolutionary platform that has been recently adopted in the clinical laboratory. The primary advantage of aCGH is that the array is capable of simultaneously detecting DNA copy changes at multiple loci over the whole genome [21].

In the present study, aCGH analysis identified gains of genomic copy numbers including *PLP1* in five subjects (P1, P2, P3, P4, P5), and the sizes of the chromosomal duplications were 374, 461, 676, 858, and 951-kb, respectively (Table 1 and Fig. 1a). The 461-kb duplication identified in P2 was not detected using standard FISH analysis at another medical facility previously, indicating the advantages of aCGH testing for PMD. There was no genomic copy number aberration in the remaining ten subjects (data not shown). A genomic copy number gain was identified on Xp22.31 with the size of 1.5-Mb in the sample from S1 (Fig. 1b).

4.3. Fiber-FISH analysis

aCGH holds the promise of being the initial diagnostic tool in the identification of visible and submicroscopic

Table 1
Clinical characteristics of the patients with PLP1 duplications or mutations.

	P1	P2	P3	P4	P5	P6	P7	P8	P9	P10
Clinical subtype	Connatal	Classic	Connatal	Connatal	Connatal	Connatal	Connatal	Connatal	Connatal	Connatal
Age at examination	1 year	14 years	20 years	4 months	2 years	2 years	1 year	1 year	4 months	1 year 5 months
Disease onset	1 month	1 day	NA	1 day	1 month	2 months	1 day	1 week	1 month	1 month
Symptoms at onset	Nystagmus	Nystagmus	NA	Nystagmus	Nystagmus Hypotonia	Nystagmus	Asphyxia	Abnormal ABR	Microcephaly*	Nystagmus
Severity score	0	2	0	0	0	0	0	0	0	0
Family history	+	None	NA	None	None	None	None	None	None	None
Age at death				4 years						
Psychomotor development										
Head control	None	7 months	None	None	None	None	None	None	None	None
Sitting	None	4 years	None	None	None	None	None	None	None	None
Walking	None	4 years	None	None	None	None	None	None	None	None
Last evaluation	14 years	14 years	33 years	4 years	2 years	2 years	1 year	4 years	5 months	1 year 5 months
Neurological signs										
Nystagmus	+	+	None	+	+	+	+	+	+	+
Muscular hypotonia	+	None	+	+	+	+ (upper limbs)	+	+	+	+
Pyramidal signs	None	+	+		+	+ (lower limbs)	None	None	None	
Ataxia		+								
Tremor	+									
Seizures				+				+	+	Sensori-neural
deafness										
Other symptoms		Dysarthria		Choreoathetosis			Strider		Microcephaly	
Disease course		Deterioration; now only sitting								
ABR findings	Only I–III waves	Only I–III waves	NA	Only I wave	Only I wave	Only I wave	Only I–III waves	Only I wave	Only I wave	Only I–II waves
MRI findings	Delayed myelination	Incomplete myelination	NA	Hypomyelination	Hypomyelination	Delayed myelination	Delayed myelination	Delayed myelination	Delayed myelination	Hypomyelination
Genotype	Duplication	Duplication	Duplication	Duplication	Duplication	Missense mutation exon 2c.149A>G(p.Tyr50Cys)	Missense mutation exon 3c.247G>A(p.Gly83Arg)	Missense mutation exon 3c.254TA>Cp.Leu85Pro	Splicing mutation intron 3IVS3-1G>C (splicing error)	Nucleotide deletion exon 3c.238_240delTTC (p.Phe80del)
	374-kb	461-kb	676-kb	858-kb	951-kb					

*, His microcephaly is −3.2SD; NA, not available; MRI, magnetic resonance imaging; ABR, auditory brain response.

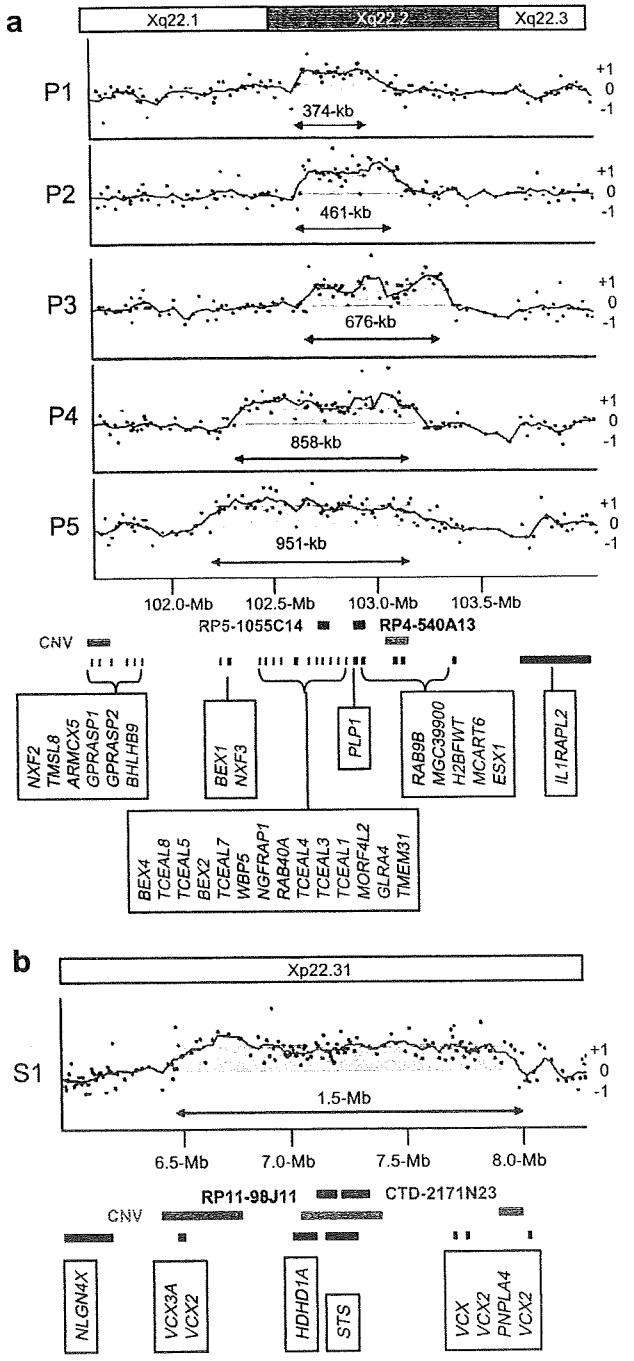

Fig. 1. Results of aCGH. CGH Analytics ver 3.5 (Agilent technologies) visualized genomic copy number aberration on Xq22.2 including *PLP1* (P1, P2, P3, P4, P5) (a) and on Xp22.31 including *STS* (S1) (b). The *X*-axis indicates physical position of chromosome X, and the scales of chromosome bands and physical position were depicted top and bottom, respectively. The *Y*-axis indicates the signal $\log_2$ ratio; positive and negative numbers indicate gain and loss of genomic copy numbers, respectively. The locations of the indicated genes (black rectangles), known copy number variations (CNVs) (orange rectangles), and the two BAC probes used in fiber-FISH analyses with green and red rectangles are shown under the figure depicted on the map according to the scale.

chromosome abnormalities [22], but it does not provide genome position or orientation information. Several cases have been reported in which the duplication is non-contiguous and the additional copy is found in a cytogenetically distinguishable band on the X chromosome (Xq22 and Xq26.3) [23]. Therefore, we should reconfirm the results of aCGH by another method including FISH analysis, especially in case of genetic counseling [23].

We checked the signals by conventional FISH analysis using metaphase, and translocations were denied in all samples (data not shown). Subsequently, two-color fiber-FISH analyses were performed to confirm the directions of the genomic duplications of *PLP1* in the five subjects, and the all duplicated segments were inserted in tandem (Fig. 2). The subjects with the longer duplicated regions (P4 and P5) showed longer intervals between the 2 sets of probe signals, which are consistent with the results of the aCGH analysis (Fig. 1a). The gain of genomic copy number on Xp22.31 in S1 was also analyzed by fiber-FISH, which showed inverted segments (Fig. 2).

Detection and visualization of *PLP1* duplications require specific molecular and cytogenetic technologies. Duplication of chromosomal regions can be determined by FISH analysis as a doublet signal in interphase chromosomes derived from immortalized lymphocyte cell lines [14,24]. However, when the duplicated region is very small and the locations of the duplicated segments are too close to each other, it is difficult to identify signals independently even if we use interphase chromosomes. In such cases, stretched chromatins rather than

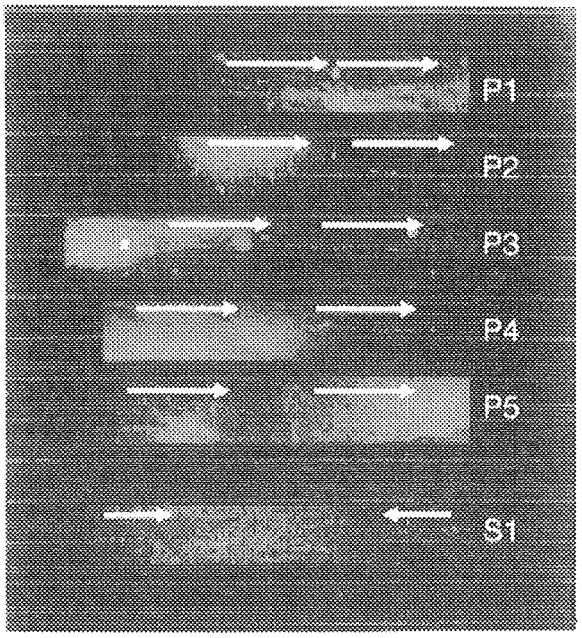

Fig. 2. The results of two-color fiber-FISH analyses. White arrows indicate the direction of duplicated segments.

the conventional interphase or metaphase chromosomes can be used for fiber-FISH analysis [25]. In this technique, two copies of the gene can be visualized as a doublet signal [14].

Interestingly, in PMD patients with *PLP1* duplications, the rearrangement breakpoints for each patient are different, yielding duplicated genomic segments of varying lengths [25–28]. Based on the genomic region around *PLP1*, Woodward et al. suggest that duplicated segments or low copy repeats (LCRs) may promote instability [26]. In this study, the distal ends of the duplicated segments were located in a copy number variation (CNV) region (cnp1417: 102,969,058–103,341,717) [29] in all five subjects, and the proximal ends were differently expanded (Fig. 1a). These findings were similar to the majority of the 11 duplications found by Woodward et al. [26]. Additional studies have shown that *PLP1* duplication events may be stimulated by LCRs or by nonhomologous pairs at both the proximal and distal breakpoints [21]. Despite the variation in size, the duplications encompassing *PLP1* are usually found in tandem [26,30]. All of our subjects with *PLP1* duplications had tandem duplications, as revealed by fiber-FISH analysis (Fig. 2). We also analyzed the region of microduplications of *STS* on Xp22.31, known as the CNV region, by fiver-FISH, which demonstrated that the duplicated segment was inserted in inverted direction (Fig. 2). This indicates that the chromosomal duplication mechanism varies depending on the location.

4.4. PLP1 mutations

To attempt to identify the genomic anomalies responsible for PMD in the remaining ten patients without *PLP1* duplications, we sequenced all the seven exons of *PLP1* and identified nucleotide alterations in five patients (Table 1, Fig. 3). Three of them were missense mutations, i.e. c.149A>G (p.Tyr50Cys) in exon 2, c.247G>A (p.Gly83Arg) in exon 3, and c.254T>C (p.Leu85Pro) in exon 3, in P6, P7, and P8, respectively. One was a splicing mutation, IVS3-1G>C in intron 3, in P9. Another was 3-bp deletion, c.238_240delCTT (p.Phe80del) in exon 3, in P10. Although c.149A>G was previously reported by Hübner et al. [18], the others were novel.

The two missense substitutions, c.247G>A and c.254T>C, are located within the second hydrophobic transmembrane domain. The nucleotide alteration, IVS3-1G>C, is located within the consensus splicing acceptor site. There is a similar known splicing mutation at the same splicing acceptor site, but it was IVS3-1G>T [31]. As PLP1 is expressed only in the central nervous system, we cannot confirm splicing alterations by RT-PCR. However, the mutations in the consensus splicing sites are believed to cause splicing abnormalities. The other novel 3-bp deletion, c.238_240delTTC, in exon 3 will cause in-frame amino acid deletion. All four novel

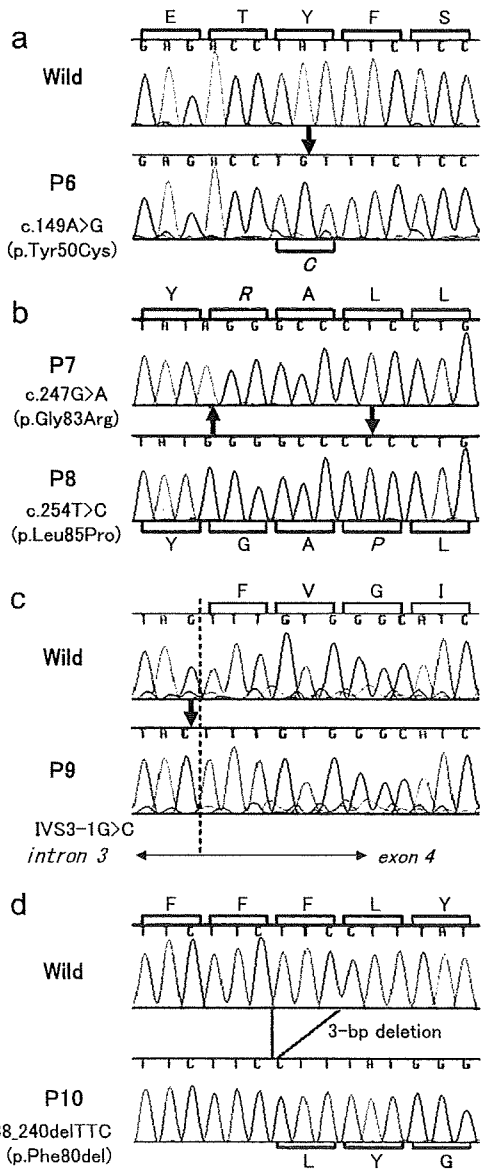

Fig. 3. Partial sequence electrophoregrams of *PLP1* mutations identified in this study. Thick arrows and italic amino acid symbols indicate the positions of mutations and altered amino acids, respectively. The broken line indicates exon–intron boundary (C). wild; sequence of wild type.

mutations were not detected in the 100 control samples, leading us to conclude that these should not be polymorphisms. Because it is well known that the genomic sequence of *PLP1* is highly conserved between species [32], these novel mutations should be pathogenic for patients with PMD. Previously, we reported two pathogenic *PLP1* mutations identified on the patients with the connatal form of PMD, and one of which, jimpy^{msd} mutation, was identical with the mice model [33,34]. Including them, more than 100 *PLP1* mutations have been reported to date (see the GeneTests Web site: http://www.genetests.org). Mutations

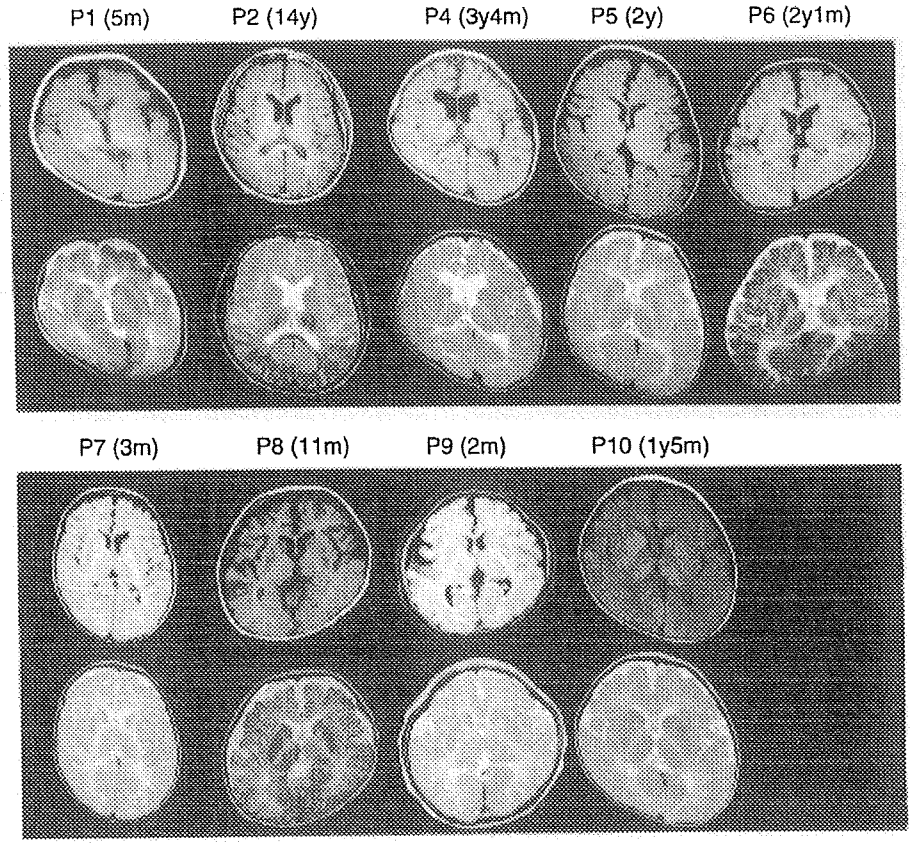

Fig. 4. Brain MRIs of nine patients analyzed in this study. Axial T1- and T2-weighted images are in the top and bottom rows, respectively. Ages at the time of examination are shown in brackets. y; years, m; months.

are distributed throughout all of the *PLP1* coding exons, and each mutation is usually unique to a family [7]. The fact that the majority of *PLP1* missense mutations cause more severe phenotypes than null mutations suggests that the profound dysmyelination resulting from *PLP1* point mutations probably arises not from the absence of functional protein, but rather from a cytotoxic effect of the mutant protein [3].

4.5. Correlation of *PLP1* genotypes with PMD phenotypes

The clinical phenotypes of ten subjects who were diagnosed as having *PLP1* duplications (five) or *PLP1* nucleotide alterations (five) are summarized in Table 1. P2 is the only patient with the milder classic form of PMD, and demonstrated the greatest walking ability of all cases in this study. The other subjects were diagnosed with the connatal form of PMD with severe developmental delay. P4 died at age 4, although no details were provided.

Brain MRIs were obtained from nine patients and shown in Fig. 4. All of them showed abnormal intensity in the white matter. Although P2 showed normal high intensity in T1-weighted image (T1), that of the frontal lobe in T2-weighted image (T2) is higher than that of the occipital. This indicated incomplete myelination. P6, P7, P8, and P9 showed high intensity in both T1 and T2, indicating delayed myelination. P1 showed low intensity in T1, and high intensity in T2. As these MRIs were obtained when he was 5 months old, this indicated delayed myelination. P4, P5, and P10 showed low intensity in T1, and high intensity in T2, indicating very severe hypomyelination.

All ten patients having a *PLP1* mutation or duplication showed nystagmus in early infancy, dysmyelination revealed by MRI, and auditory brain response (ABR) abnormalities (Table 1). This triad of presenting symptoms should be the clue to get a clinical diagnosis of PMD. Regarding the radiological findings of the patients, all the provided MRI findings showed dysmyelination with varying degrees (Fig. 4). P4 with the most severe phenotype of PMD showed very low intensity white matter in the T1-weighted imaging, whereas P2 with the mildest form of PMD showed only mildly affected incomplete myelination in T2-weighted imaging. These MRI findings are well-correlated with the clinical severity.

All five patients with nucleotide alterations in *PLP1* displayed the very severe connatal type PMD, whereas P2 whose genome contained a small duplication including *PLP1* showed the milder classical type PMD. These results agree with previous reports showing that the phe-

notypes of patients with genomic duplications are generally milder than those with nucleotide mutations [3]. However, the other four patients with *PLP1* duplications, P1, P3, P4, and P5, displayed the severe connatal form of PMD.

P4 showed a large duplicated region and died when he was 4 years old. On the other hand, P1 contained a very small duplicated segment, similar to P2 in the length, but displayed a very severe phenotype. Thus, it appears that, as suggested by Regis et al., the extent of the duplicated genomic segments does not correlate with clinical severity [35].

According to Lee et al., 65% of patients with *PLP1* duplications have complex rearrangements in nucleotide sequence levels [28]. In this study, we detected *PLP1* duplications by aCGH, and the directions of those duplicated regions were determined by fiber-FISH. However, there is still the possibility that more complicated small rearrangements exist in the duplicated region, particularly in P1. The existence of more complicated rearrangements may explain the reason why there is no correlation between the size of the duplication and the phenotypic severity.

4.6. Differential diagnosis

After genetic evaluation of *PLP1*, the five patients, who did not show any mutations in *PLP1*, were re-evaluated, and one of them was diagnosed as having metachromatic leukodystrophy in the other institution. Another patient showed congenital leukodystrophy with migrating partial seizures in infancy, but no nystagmus and no ABR abnormality, indicating that PMD would be misdiagnosis. Since the other three patients fulfilled the triad described above, the disease-causing mutations might be on the non-coding upstream region of PLP1, or on the other candidate genes for congenital leukodystrophy, including the gap junction protein α12 (GJA12) and others [36,37].

Acknowledgements

This work was supported by the International Research and Educational Institute for Integrated Medical Sciences, Tokyo Women's Medical University, which is supported by the Program for Promoting the Establishment of Strategic Research Centers, Special Coordination Funds for Promoting Science and Technology, Ministry of Education, Culture, Sports, Science and Technology (Japan).

References

[1] Boulloche J, Aicardi J. Pelizaeus–Merzbacher disease: clinical and nosological study. J Child Neurol 1986;1:233–9.
[2] Koeppen AH, Robitaille Y. Pelizaeus–Merzbacher disease. J Neuropathol Exp Neurol 2002;61:747–59.
[3] Inoue K. PLP1-related inherited dysmyelinating disorders: Pelizaeus–Merzbacher disease and spastic paraplegia type 2. Neurogenetics 2005;6:1–16.
[4] Hudson LD, Puckett C, Berndt J, Chan J, Gencic S. Mutation of the proteolipid protein gene PLP in a human X chromosome-linked myelin disorder. Proc Natl Acad Sci USA 1989;86:8128–31.
[5] Gencic S, Abuelo D, Ambler M, Hudson LD. Pelizaeus–Merzbacher disease: an X-linked neurologic disorder of myelin metabolism with a novel mutation in the gene encoding proteolipid protein. Am J Hum Genet 1989;45:435–42.
[6] Ellis D, Malcolm S. Proteolipid protein gene dosage effect in Pelizaeus–Merzbacher disease. Nat Genet 1994;6:333–4.
[7] Garbern JY. Pelizaeus–Merzbacher disease: genetic and cellular pathogenesis. Cell Mol Life Sci 2007;64:50–65.
[8] Heim P, Claussen M, Hoffmann B, Conzelmann E, Gartner J, Harzer K, et al. Leukodystrophy incidence in Germany. Am J Med Genet 1997;71:475–8.
[9] Cailloux F, Gauthier-Barichard F, Mimault C, Isabelle V, Courtois V, Giraud G, et al. Genotype-phenotype correlation in inherited brain myelination defects due to proteolipid protein gene mutations. Clinical European network on brain dysmyelinating disease. Eur J Hum Genet 2000;8:837–45.
[10] Sistermans EA, de Coo RF, De Wijs IJ, Van Oost BA. Duplication of the proteolipid protein gene is the major cause of Pelizaeus–Merzbacher disease. Neurology 1998;50:1749–54.
[11] Mimault C, Giraud G, Courtois V, Cailloux F, Boire JY, Dastugue B, et al. Proteolipoprotein gene analysis in 82 patients with sporadic Pelizaeus–Merzbacher disease: duplications, the major cause of the disease, originate more frequently in male germ cells, but point mutations do not. The clinical European network on brain dysmyelinating disease. Am J Hum Genet 1999;65:360–9.
[12] Caro PA, Marks HG. Magnetic resonance imaging and computed tomography in Pelizaeus–Merzbacher disease. Magn Reson Imaging 1990;8:791–6.
[13] Inoue K, Osaka H, Sugiyama N, Kawanishi C, Onishi H, Nezu A, et al. A duplicated PLP gene causing Pelizaeus–Merzbacher disease detected by comparative multiplex PCR. Am J Hum Genet 1996;59:32–9.
[14] Woodward K, Kendall E, Vetrie D, Malcolm S. Pelizaeus–Merzbacher disease: identification of Xq22 proteolipid-protein duplications and characterization of breakpoints by interphase FISH. Am J Hum Genet 1998;63:207–17.
[15] Wolf NI, Sistermans EA, Cundall M, Hobson GM, Davis-Williams AP, Palmer R, et al. Three or more copies of the proteolipid protein gene PLP1 cause severe Pelizaeus–Merzbacher disease. Brain 2005;128:743–51.
[16] Combes P, Bonnet-Dupeyron MN, Gauthier-Barichard F, Schiffmann R, Bertini E, Rodriguez D, et al. PLP1 and GPM6B intragenic copy number analysis by MAPH in 262 patients with hypomyelinating leukodystrophies: identification of one partial triplication and two partial deletions of PLP1. Neurogenetics 2006;7:31–7.
[17] Lee JA, Cheung SW, Ward PA, Inoue K, Lupski JR. Prenatal diagnosis of PLP1 copy number by array comparative genomic hybridization. Prenat Diagn 2005;25:1188–91.
[18] Hubner CA, Orth U, Senning A, Steglich C, Kohlschutter A, Korinthenberg R, et al. Seventeen novel PLP1 mutations in patients with Pelizaeus–Merzbacher disease. Hum Mutat 2005;25:321–2.
[19] Bartocci A, Striano P, Mancardi MM, Fichera M, Castiglia L, Galesi O, et al. Partial monosomy Xq(Xq23 –> qter) and trisomy 4p(4p15.33 –> pter) in a woman with intractable focal epilepsy, borderline intellectual functioning, and dysmorphic features. Brain Dev 2008;30:425–9.
[20] Hobson GM, Davis AP, Stowell NC, Kolodny EH, Sistermans EA, de Coo IF, et al. Mutations in noncoding regions of the proteolipid protein gene in Pelizaeus–Merzbacher disease. Neurology 2000;55:1089–96.

[21] Bejjani BA, Shaffer LG. Application of array-based comparative genomic hybridization to clinical diagnostics. J Mol Diagn 2006;8:528–33.
[22] Shaffer LG, Bejjani BA. Medical applications of array CGH and the transformation of clinical cytogenetics. Cytogenet Genome Res 2006;115:303–9.
[23] Woodward K, Cundall M, Palmer R, Surtees R, Winter RM, Malcolm S. Complex chromosomal rearrangement and associated counseling issues in a family with Pelizaeus–Merzbacher disease. Am J Med Genet A 2003;118A:15–24.
[24] Inoue K, Kanai M, Tanabe Y, Kubota T, Kashork CD, Wakui K, et al. Prenatal interphase FISH diagnosis of PLP1 duplication associated with Pelizaeus–Merzbacher disease. Prenat Diagn 2001;21:1133–6.
[25] Inoue K, Osaka H, Imaizumi K, Nezu A, Takanashi J, Arii J, et al. Proteolipid protein gene duplications causing Pelizaeus–Merzbacher disease: molecular mechanism and phenotypic manifestations. Ann Neurol 1999;45:624–32.
[26] Woodward KJ, Cundall M, Sperle K, Sistermans EA, Ross M, Howell G, et al. Heterogeneous duplications in patients with Pelizaeus–Merzbacher disease suggest a mechanism of coupled homologous and nonhomologous recombination. Am J Hum Genet 2005;77:966–87.
[27] Lee JA, Inoue K, Cheung SW, Shaw CA, Stankiewicz P, Lupski JR. Role of genomic architecture in PLP1 duplication causing Pelizaeus–Merzbacher disease. Hum Mol Genet 2006;15:2250–65.
[28] Lee JA, Carvalho CM, Lupski JR. A DNA replication mechanism for generating nonrecurrent rearrangements associated with genomic disorders. Cell 2007;131:1235–47.
[29] Redon R, Ishikawa S, Fitch KR, Feuk L, Perry GH, Andrews TD, et al. Global variation in copy number in the human genome. Nature 2006;444:444–54.
[30] Inoue K. Pelizaeus–Merzbacher disease and spastic paraplegia type 2. In: Lupski JR, Stankiewicz P, editors. Genomic disorders. Totowa, NJ: Humana press; 2006. p. 263–9.
[31] Strautnieks S, Malcolm S. A G to T mutation at a splice site in a case of Pelizaeus–Merzbacher disease. Hum Mol Genet 1993;2:2191–2.
[32] Diehl HJ, Schaich M, Budzinski RM, Stoffel W. Individual exons encode the integral membrane domains of human myelin proteolipid protein. Proc Natl Acad Sci USA 1986;83:9807–11.
[33] Yamamoto T, Nanba E, Zhang H, Sasaki M, Komaki H, Takeshita K. Jimpy(msd) mouse mutation and connatal Pelizaeus–Merzbacher disease. Am J Med Genet 1998;75:439–40.
[34] Yamamoto T, Nanba E. A novel mutation (A246T) in exon 6 of the proteolipid protein gene associated with connatal Pelizaeus–Merzbacher disease. Hum Mutat 1999;14:182.
[35] Regis S, Biancheri R, Bertini E, Burlina A, Lualdi S, Bianco MG, et al. Genotype-phenotype correlation in five Pelizaeus–Merzbacher disease patients with PLP1 gene duplications. Clin Genet 2008;73:279–87.
[36] Uhlenberg B, Schuelke M, Ruschendorf F, Ruf N, Kaindl AM, Henneke M, et al. Mutations in the gene encoding gap junction protein alpha 12 (connexin 46.6) cause Pelizaeus–Merzbacher-like disease. Am J Hum Genet 2004;75:251–60.
[37] Henneke M, Combes P, Diekmann S, Bertini E, Brockmann K, Burlina AP, et al. GJA12 mutations are a rare cause of Pelizaeus–Merzbacher-like disease. Neurology 2008;70:748–54.

ELSEVIER

Case Reports

Three Patients With Severe Bilateral Frontoparietal Polymicrogyria

Tomohiro Nakayama, MD, Hirokazu Oguni, MD, Makoto Funatsuka, MD, Kayoko Saito, MD, and Makiko Osawa, MD

The bilateral frontoparietal polymicrogyria syndrome is characterized anatomically by predominantly frontoparietal diffuse polymicrogyria and clinically by generalized tonic-clonic seizures and mental retardation developing in early childhood. Despite the diffuse nature of the cortical involvement, patients do gain the ability to speak and to walk. In addition, epilepsy can be relatively well controlled with antiepileptic drugs. In three cases of bilateral frontoparietal polymicrogyria, the patients demonstrated consistently similar clinical and neuroimaging characteristics, with more severe structural and developmental abnormalities than those reported previously. The designation proposed here recognizes such cases as a severe form of bilateral frontoparietal polymicrogyria. An ethnic difference or a causal gene other than *GPR56* might be responsible for the difference in severity between the classical and the more severe forms of bilateral frontoparietal polymicrogyria.

Nakayama T, Oguni H, Funatsuka M, Saito K, Osawa M. Three patients with severe bilateral frontoparietal polymicrogyria. Pediatr Neurol 2008;38:353-356.

Introduction

Polymicrogyria is one of the developmental brain anomalies that give rise to cortical disorganization in the late fetal period. Since the advent of high resolution magnetic resonance imaging, various forms of diffuse or focal polymicrogyria have been reported, among which bilateral frontoparietal polymicrogyria is a specific form of diffuse polymicrogyria delineated clinically and genetically by Piao et al. [1]. It is characterized anatomically by predominantly frontoparietal diffuse polymicrogyria and clinically by generalized tonic-clonic seizures and mental retardation developing in early childhood. Despite the diffuse widespread nature of the cortical involvement, patients do gain the abilities to speak and walk but are always mentally retarded. In addition, epilepsy can be relatively well controlled by antiepileptic drugs. The causal gene, *GPR56*, was recently identified, by means of familial linkage analysis; located on chromosome segment 16q12.2~21, *GPR56* encodes one of the G protein binding receptors [2,3].

Reported here are three cases of bilateral frontoparietal polymicrogyria, each with a consistent clinical picture with unusually severe structural and developmental abnormalities, compared with those reported previously. Based on these three cases, a new designation is proposed, that of a severe form of bilateral frontoparietal polymicrogyria.

Subjects and Methods

The three subjects were Japanese boys, whose bilateral frontoparietal polymicrogyria was confirmed by cranial magnetic resonance imaging. Their ages at diagnosis were 11 months, 2 years 7 months, and 5 years 7 months. Medical records and electroencephalography and magnetic resonance imaging findings were analyzed retrospectively. Cranial magnetic resonance imaging was performed with a 1.5 T Signa MR unit (GE Healthcare, Wauwatosa, WI). For each patient, examinations included T_1-weighted, T_2-weighted, and fluid-attenuated inversion-recovery (FLAIR) images in the axial plane.

From Department of Pediatrics, School of Medicine, Tokyo Women's Medical University, Tokyo, Japan.

Communications should be addressed to:
Dr. Nakayama; Department of Pediatrics; Tokyo Women's Medical University; 8-1, Kawada-cho, Shinjuku-ku; Tokyo 162-8666; Japan.
E-mail: tonaka@ped.twmu.ac.jp
Received May 2, 2007; accepted December 28, 2007.

doi:10.1016/j.pediatrneurol.2007.12.013 • 0887-8994/08/$—see front matter

Case Reports

Case 1

The first patient is a boy, 2 years 9 months old at diagnosis. There were no convulsive disorders in his family history. He had been born at 38 weeks and 2 days gestational age, with an uneventful delivery, of nonconsanguineous parents. At birth, microcephaly was noted, with a head circumference of 28.0 cm (−3.9 standard deviations). Neither prenatal infections nor any known congenital defects of metabolism were detected. At 3 months of age, he developed epileptic spasms in clusters, and was referred to the Tokyo Women's Medical University hospital.

Physical examination yielded no remarkable findings except for microcephaly. Neurologic examination revealed marked spasticity in all four limbs with exaggerated deep tendon reflexes. Electroencephalography revealed the periodic appearance of diffuse irregular spikes or spike and wave complexes during wakefulness and sleep, findings compatible with hypsarrhythmia. Cranial magnetic resonance imaging revealed frontoparietal predominant diffuse and bilaterally symmetric polymicrogyria with ventricular dilatation (Fig 1a). With the diagnosis of symptomatic West syndrome, the patient was started on antiepileptic drug treatment with valproate, zonisamide, and vitamin B6, but no effect was obtained. The patient did, however, respond well to adrenocorticotropic hormone therapy. As of writing, he had been seizure free on a combination of valproate (30 mg/kg/day) and clonazepam (0.04 mg/kg/day) since the adrenocorticotropic hormone therapy. He never achieved head control or visual following, and remained unable to speak or sit up.

Case 2

The second patient is a boy, 2 years 7 months old at diagnosis. There were no convulsive disorders in his family history. He had been born to nonconsanguineous parents and was delivered uneventfully at 41 weeks and 4 days gestational age. At 4 months of age, he developed epileptic seizures in clusters and hypsarrhythmia, and was diagnosed at a local hospital as having West syndrome. Epileptic episodes were ultimately controlled by zonisamide (15 mg/kg/day), after he proved to be resistant to vitamin B6, valproate (55 mg/kg/day), and adrenocorticotropic hormone therapy. At 9 months of age, he experienced acute respiratory failure due to adenovirus pneumonia, requiring steroid pulse therapy, gamma globulin therapy, and artificial ventilation. At the age of 1 year and 3 months, he was referred to Tokyo Women's Medical University hospital for surgical correction of gastroesophageal reflux.

Physical findings revealed a well-nourished boy without microcephaly. Neurologic examination revealed marked spasticity in all four limbs, with exaggerated deep tendon reflexes and ankle clonus. Electroencephalography revealed diffuse moderately slow background activity with intermittent bilateral frontal spikes. Cranial magnetic resonance imaging revealed frontoparietal predominant diffuse and bilaterally symmetrical polymicrogyria with ventricular dilatation identical to that of the cases 1 and 3.

Case 3

The third patient is a boy, 7 years 5 months old at diagnosis. Born at 39 weeks gestational age, to nonconsanguineous parents, he had been delivered uneventfully. There were no convulsive disorders in his family history. Since birth, he had repeatedly experienced episodes of choking whenever he was fed milk. At 3 months of age, he developed attacks characterized by sudden turning of the head after repetitive blinking. At 6 months of age, generalized tonic seizures and myoclonic attacks appeared. He was referred to Tokyo Women's Medical University hospital at the age of 1 year 6 months.

On admission, no more than one generalized tonic seizure was occurring in a month, and myoclonic seizures occurred 10 times a day. Physically, he was a well-nourished boy but breathed with some stridor. Neurological examination revealed marked spasticity in all four limbs with exaggerated deep tendon reflexes. Electroencephalography revealed intermittent spike discharges recorded from the left frontal region. Cranial magnetic resonance imaging revealed frontoparietal predominant diffuse and bilaterally symmetrical polymicrogyria (Fig 1b). The epilep-

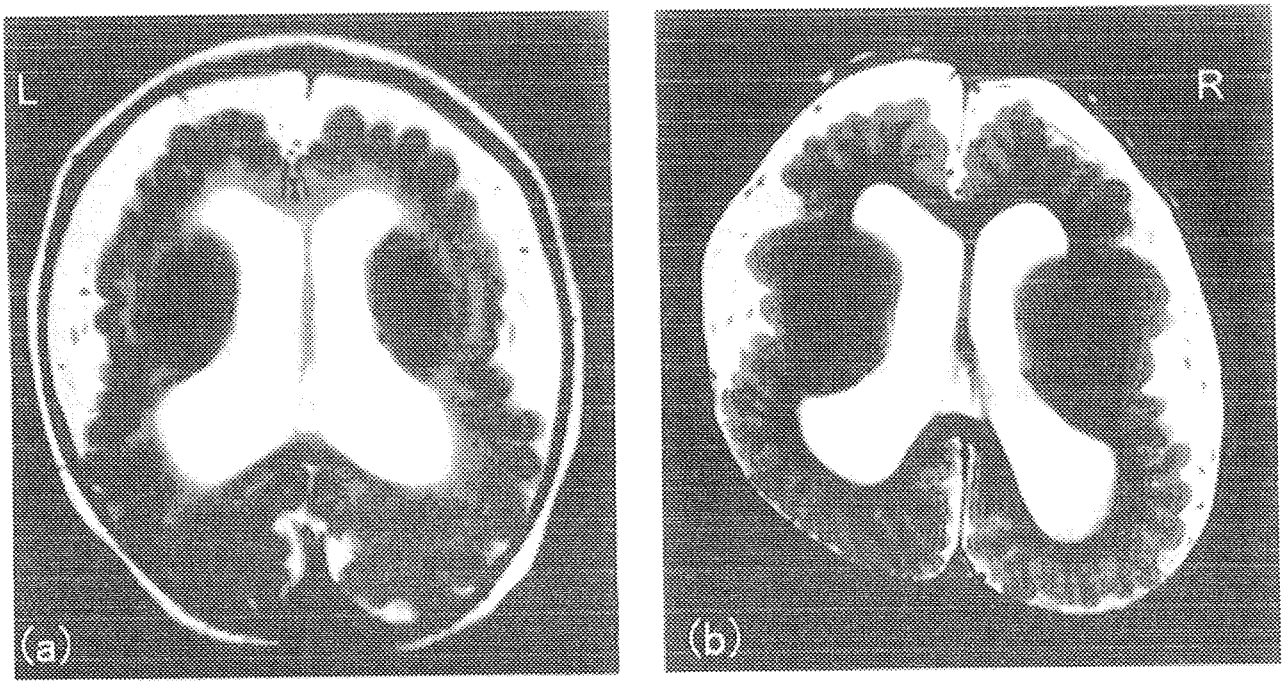

Figure 1. Axial T_2-weighted cranial magnetic resonance imaging reveals an irregularly bumpy appearance for almost the entire cortical surface, indicating frontoparietal predominant diffuse and bilaterally symmetric polymicrogyria in both cases. Also notable are enlarged cerebrospinal fluid space over both frontoparietal regions, enlarged lateral ventricles, and markedly reduced white matter volume. (a) Case 1 at 6 months of age (TR/TE = 4000/98 ms). (b) Case 3 at 3 years 10 months of age (TR/TE = 6500/45 ms).

tic seizures were relatively well controlled by a combination of valproate (35 mg/kg/day) and clonazepam (0.01 mg/kg/day).

At 2 years and 2 months of age, he experienced acute respiratory failure due to adenovirus pneumonia, which required steroid pulse therapy, gamma globulin therapy, and artificial ventilation. The residual pulmonary damage was serious, and both tracheotomy and chronic artificial ventilatory assistance have since been required. Although, as of writing, he had been seizure free for more than 3 years, he lacked head control and visual following, and could neither speak nor sit up.

Results

These three Japanese boys had diffuse bilateral frontoparietal lobe dominant polymicrogyria and ventricular dilatation evident upon magnetic resonance imaging. Two of the patients developed epileptic spasms in clusters (one at age 3 months, the other at age 4 months), controlled by adrenocorticotropic hormone therapy. All three boys were severely disabled, and never achieved head control, speaking, sitting, or visual following (Table 1).

The laboratory examinations included a chromosomal study, routine blood and urinary examinations, urinary organic and amino acid screening, and cerebrospinal fluid lactate testing. The findings were within normal range in all three patients.

Discussion

Polymicrogyria is a relatively common malformation of cortical development, in which the brain surface is irregular and the normal gyral pattern is replaced by an excessive number of small and partly fused gyri separated by shallow sulci [4]. In the past, the diagnosis of polymicrogyria has been confounded with pachygyria and schizencephalic clefts; however, advancements in imaging studies have improved the diagnosis and classification of this condition, and it is now possible to delineate several region-specific polymicrogyria syndromes. Barkovich et al. [5] classified polymicrogyrias and schizencephalies into four categories: (1) bilateral polymicrogyria syndromes, (2) schizencephaly, (3) schizencephaly and polymicrogyria with other brain malformations or abnormalities, and (4) polymicrogyria and schizencephaly as part of a syndrome termed multiple congenital anomaly/mental retardation. They further subclassified these four categories into 15 subgroups, 5 of them applying to the polymicrogyria syndromes: (1) bilateral diffuse polymicrogyria, (2) bilateral frontal polymicrogyria, (3) bilateral perisylvian polymicrogyria, (4) bilateral parieto-occipital polymicrogyria, and (5) bilateral mesial occipital polymicrogyria.

Several reports of the syndrome of bilateral frontoparietal polymicrogyria are available [1-3,6-8]. Piao et al. [1,2] conducted an extensive clinical and genetic study of 19 bilateral frontoparietal polymicrogyria patients, who were mainly of Middle Eastern origin and had consanguineous parents. These patients had generalized tonic-clonic seizures from early childhood, which were easily controlled by antiepileptic drugs. Although all were moderately retarded, they acquired a few words, and ambulation [1,2] (Table 1).

The pathogenesis underlying the development of polymicrogyria and the regional distribution of polymicrogyria

Table 1. Clinical characteristics of the present three cases of bilateral frontoparietal polymicrogyria, compared with published cases

Characteristic	Chang et al. [3]	Case 1	Case 2	Case 3
Ethnicity	Palestinian, Afghani, Pakistani, Qatari, and others of Middle Eastern origin	Japanese	Japanese	Japanese
Consanguinity	Present	Absent	Absent	Absent
Sex	Male, female	Male	Male	Male
Age at diagnosis	Not available	2 yr 11 mo	2 yr 7 mo	5 yr 7 mo
Head circumference	Microcephaly in 3 of 19; otherwise normal	Microcephaly	Normal	Normal
Cerebral palsy	Not available	Quadriplegia	Quadriplegia	Quadriplegia
Pyramidal sign	Present	Present	Present	Present
Visual response	Present	Absent	Absent	Absent
Developmental delay	Moderate	Severe	Severe	Severe
Motor function	Ambulatory	Bedridden	Bedridden	Bedridden
Gastrointestinal symptoms	Not available	Absent	Gastroesophageal reflux	Gastroesophageal reflux
Blood, cerebrospinal fluid, and urine examination	Not available	Normal	Normal	Normal
Electroencephalography findings	Not available	Hypsarrhythmia	Slow background activity	Sporadic frontal spike
Seizure onset	Early childhood	3 mo	4 mo	3 mo
Seizure type	Generalized tonic-clonic	West syndrome	West syndrome	Myoclonic, generalized tonic
Treatment	Antiepileptic drugs	valproate, zonisamide	Vitamin B6, valproate, zonisamide	Valproate, clobazam, zonisamide, clonazepam
Adrenocorticotropic hormone therapy	No	Yes	Yes	No
Seizure-free period	13 mo to 29 yr	6 mo	2 yr	1 yr 3 mo

remain undetermined. Mitchell et al. [9] reported a mother and her son with unilateral polymicrogyria caused by a mutation of the paired-box transcription factor, PAX6, which was demonstrated in murine models. Piao et al. [1] identified the causative gene of bilateral frontoparietal polymicrogyria as the G protein-coupled receptor gene 6, *GPR56*, which was expressed on the leading edge of membrane filopodia of human glioma cells and colocalized with α-actinin [10]. Purified recombinant GPR56 extracellular domain protein inhibited cell adhesion and caused abnormal cytoskeletal morphology and cell rounding. These findings indicated that the GPR56 protein is involved in adhesion signaling and plays an essential role in regional patterning of the human cortex. Given, however, that polymicrogyria itself is associated with many known genetic disorders, including chromosomal 22q11 deletion syndromes [11], mtDNA point mutation [12], and Ehlers-Danlos syndrome [13], other factors must be involved in the pathogenesis.

In the present three cases, the anatomic structure of the brain showed more severe diffuse cortical and subcortical involvements than those seen in the bilateral frontoparietal polymicrogyria cases previously reported by Piao et al. [1,2] and others [6-8]. All three sporadic in origin, and there were no convulsive disorders in their families. Convulsions started during early infancy in the form of myoclonic seizures or spasms in clusters. Two patients developed West syndrome, which was successfully controlled. The third patient had myoclonic seizures and generalized tonic seizures with severe background EEG abnormalities and multiple epileptic EEG foci, which were also controlled by antiepileptic drugs. All three patients had quadriplegic cerebral palsy and profound retardation; none of them achieved head control, speaking, sitting, or visual following.

The three patients exhibited consistently similar clinical and neuroimaging characteristics, with more severe structural and developmental abnormalities than those of the bilateral frontoparietal polymicrogyria cases previously reported by Piao et al. [1,2]. Although molecular analysis has not yet been performed, an ethnic difference or a causal gene other than *GPR56* might have contributed to the severity of the disease in these three patients. The designation proposed here recognizes such cases as a severe form of bilateral frontoparietal polymicrogyria. Accumulation of more cases can be expected to shed further light on this rare syndrome.

References

[1] **Piao** X, Hill RS, Bodell A, et al. G protein-coupled receptor-dependent development of human frontal cortex. Science 2004;303: 2033-6.

[2] **Piao** X, Basel-Vanagaite L, Straussberg R, et al. An autosomal recessive form of bilateral frontoparietal polymicrogyria maps to chromosome 16q12.2-21. Am J Hum Genet 2002;70:1028-33.

[3] **Chang** BS, Piao X, Bodell A, et al. Bilateral frontoparietal polymicrogyria: clinical and radiological features in 10 families with linkage to chromosome 16. Ann Neurol 2003;53:596-606.

[4] **Crome** L. Microgyria. J Pathol Bacteriol 1952;64:479-95.

[5] **Barkovich** AJ, Kuzniecky RI, Jackson GD, Guerrini R, Dobyns WB. Classification system for malformations of cortical development: update 2001. Neurology 2001;57:2168-78.

[6] **Straussberg** R, Gross S, Amir J, Gadoth N. A new autosomal recessive syndrome of pachygyria. Clin Genet 1996;50:498-501.

[7] **Sztriha** L, Nork M. Bilateral symmetrical frontoparietal polymicrogyria. Eur J Paediatr Neurol 2002;6:229-32.

[8] **Sztriha** L, Nork M. Bilateral frontoparietal polymicrogyria and epilepsy. Pediatr Neurol 2000;22:240-3.

[9] **Mitchell** TN, Free SL, Williamson KA, et al. Polymicrogyria and absence of pineal gland due to *PAX6* mutation. Ann Neurol 2003;53: 658-63.

[10] **Shashidhar** S, Lorente G, Nagavarapu U, et al. GPR56 is a GPCR that is overexpressed in gliomas and functions in tumor cell adhesion. Oncogene 2005;24:1673-82.

[11] **Bingham** PM, Lynch D, McDonald-McGinn D, Zackai E. Polymicrogyria in chromosome 22 deletion syndrome. Neurology 1998; 51:1500-2.

[12] **Keng** WT, Pilz DT, Minns B, FitzPatrick DR. A3243G mitochondrial mutation associated with polymicrogyria. Dev Med Child Neurol 2003;45:704-8.

[13] **Echaniz-Laguna** A, de Saint-Martin A, Lafontaine AL, et al. Bilateral focal polymicrogyria in Ehlers-Danlos syndrome. Arch Neurol 2000;57:123-7.

Journal of Human Genetics (2009) 54, 94–97

www.nature.com/jhg

ORIGINAL ARTICLE

Neurofilament light chain polypeptide gene mutations in Charcot–Marie–Tooth disease: nonsense mutation probably causes a recessive phenotype

Akiko Abe[1], Chikahiko Numakura[1], Kayoko Saito[2], Hiroyoshi Koide[3], Nobuyuki Oka[4], Akira Honma[5], Yumiko Kishikawa[1] and Kiyoshi Hayasaka[1]

The neurofilament light chain polypeptide (NEFL) forms the major intermediate filament in neurons and axons. *NEFL* mutation is a cause of axonal or demyelinating forms of dominant Charcot–Marie–Tooth disease (CMT). We investigated *NEFL* in 223 Japanese CMT patients who were negative for *PMP22*, *MPZ*, *GJB1*, *LITAF*, *EGR2*, *GDAP1*, *MTMR2* and *PRX* in the demyelinating form and negative for *MFN2*, *MPZ*, *GJB1*, *HSP27*, *HSP22* and *GARS* in the axonal form. We detected four heterozygous missense mutations—Pro8Leu, Glu90Lys, Asn98Ser and Glu396Lys—in five unrelated patients and a homozygous nonsense mutation, Glu140Stop, in one other patient. All patients had mildly to moderately delayed nerve conduction velocities, possibly caused by a loss of large diameter fibers. This is the first report of a homozygous nonsense mutation of *NEFL*. Results of our study show that nonsense *NEFL* mutations probably cause a recessive phenotype, in contrast to missense mutations, which cause a dominant phenotype.
Journal of Human Genetics (2009) **54**, 94–97; doi:10.1038/jhg.2008.13; published online 16 January 2009

Keywords: Charcot–Marie–Tooth disease; NEFL; neurofilament

INTRODUCTION

Charcot–Marie–Tooth disease (CMT) is the most common inherited peripheral neuropathy affecting motor and sensory nerves of the peripheral nervous system.[1] The disease has been classified into demyelinating and axonal forms based on nerve conduction velocities (NCVs). More than 26 genes have been identified as disease-causing genes of CMT (http://www.molgen.ua.ac.be/CMTMutations/Mutations). As a disease-causing genes of demyelinating forms, genes coding for myelin membrane proteins and proteins associated with the biology of Schwann's cells, including transcriptional proteins involved in the differentiation and development of Schwann's cells, have been identified. Regarding the axonal forms, genes coding for cytoskeletal proteins and proteins involved in axonal transport have been identified. A close relationship exists between axon and myelin forms: mutations of several genes are known to be associated with both forms.

The neurofilament light chain polypeptide (NEFL) is a constituent of neurofilaments: the major intermediate filament of neurons and axons. It plays a pivotal role in the assembly and maintenance of the axonal cytoskeleton.[2,3] Neurofilaments determine the axonal diameter and the conduction velocity of peripheral nerves.[4–6] Mutations of *NEFL* were reported in an autosomal-dominant axonal form of CMT type 2E (CMT2E) and[7] then in an autosomal-dominant demyelinating form of CMT type 1F (CMT1F).[8]

We investigated the frequency and phenotypic effects of *NEFL* mutations in a cohort of 223 Japanese CMT patients, including those with unclassified types. We detected four heterozygous missense mutations in five patients and a homozygous nonsense mutation in one other patient. Herein, we present discussion of the genotype–phenotype relation.

PATIENTS AND METHODS

Patients

We studied 223 unrelated CMT patients. On the basis of electrophysiological criteria, 121 patients were diagnosed with demyelinating CMT (motor median NCVs $<38\,m\,s^{-1}$), 93 patients had axonal CMT (motor median NCVs $>38\,m\,s^{-1}$) and 9 patients had unclassified CMT types.[9] The latter group included patients whose detailed results of electrophysiological investigations were not available. The patients with demyelinating and unclassified CMT were all negative on mutation screening for *PMP22*, *MPZ*, *GJB1*, *LITAF*, *EGR2*, *GDAP1*, *MTMR2* and *PRX*. The patients with axonal and unclassified types were negative for *MFN2*, *MPZ*, *GJB1*, *HSP27*, *HSP22* and *GARS*. As controls for sequence variations, 100 healthy Japanese people were screened.

[1]Department of Pediatrics, Yamagata University School of Medicine, Yamagata, Japan; [2]Institute of Medical Genetics, Tokyo Women's Medical University, Tokyo, Japan; [3]Hallo Clinic, Saitama, Japan; [4]NHO Minami-Kyoto Hospital, Kyoto, Japan and [5]Honma Child Clinic, Yamagata, Japan
Correspondence: Professor K Hayasaka, Department of Pediatrics, Yamagata University School of Medicine, 2-2-2 Iidanishi, Yamagata 990-9585, Japan.
E-mail: hayasaka@med.id.yamagata-u.ac.jp
Received 2 September 2008; revised 21 November 2008; accepted 7 December 2008; published online 16 January 2009